ELSEVIER

Polymer 42 (2001) 1219–1226

polymer

www.elsevier.nl/locate/polymer

Dynamic mechanical properties of metallocene catalyzed linear polyethylenes

K.-h. Nitta[a,*], A. Tanaka[b]

[a]School of Materials Science, Japan Advanced Institute of Science and Technology, 1-1 Asahidai, Tatsunokuchi, Ishikawa 923-1292, Japan
[b]Department of Materials Science, University of Shiga Prefecture 2500 Hassaka, Hikone, Shiga 522-8533, Japan

Received 4 January 2000; received in revised form 17 May 2000; accepted 3 June 2000

Abstract

We have examined dynamic mechanical properties of metallocene catalyzed linear polyethylenes (L-PEs) with various molecular weight M_w from ca. 20M to 2.6G and branched linear polyethylenes (B-PEs) having various degree of short-chain branching. The dynamic mechanical relaxation mechanisms of these metallocene catalyzed PE samples were discussed in the terms of the structural factors such as lamellar thickness, amorphous layer thickness, and crystallinity. It was found that the positions of α (crystal) relaxation and melting temperature have similar functional dependence of the inverse of the lamellar thickness $1/L_c$. The β relaxation appeared around 250 K in the dynamic mechanical spectra for higher molecular weight PEs having more than about 200M of M_w. The molecular mechanism underlying β relaxation for L-PE was found to be different from that for B-PE.

Keywords: Polyethylene; Metallocene; Dynamic mechanical properties

1. Introduction

The relaxation behavior of polyethylene is strongly influenced by variables that describe the crystalline-amorphous state, such as crystallinity, lamellar thickness, and amorphous layer thickness [1–5]. Three relaxations are observed, identified conventionally as α, β, and γ in order of decreasing temperature: the α relaxation is observed in the range between room temperature and melting temperature; the β relaxation is observed in the temperature range from 220 to 300 K, and the γ relaxation is in the narrow temperature range from 130 to 180 K.

The α relaxation is universally observed in all crystalline polymers. The relaxation intensifies with increasing crystallinity so that it is usually assigned to the motion of chain units within the crystalline portion. Numerous investigators [6–12] demonstrated that the α relaxation in polyethylenes consists of two overlapping peaks designated as the α_1 and α_2 relaxations in order of descending temperature. The α_1 relaxation is attributed to an intralamellar slip process (or grain boundary phenomena) and/or motion in the intercrystalline region, and the α_2 relaxation is to intracrystalline chain motion involving α transitional motion of chain segments along the *c*-axis within the crystal lattice [8]. Moreover, Takayanagi et al. [12] found that the location of the α_2 relaxation agrees with the onset temperature of thermal expansion of the α-axis spacing, suggesting that the α_2 dispersion process is caused by the incoherent interaction between crystal stems. Mansfield and Boyd have proposed that the dielectric α process can be represented by the propagation process of α twisted defect along the chain within crystal lattice, leading to reorganization of the crystal surface [13,14].

As described above, most investigators have concluded that the α relaxation arises from the crystalline phases of the semicrystalline polymers, whereas several conflicting interpretations have been given concerning the origin and molecular nature of the β and γ relaxations. Pechhold et al. [15] and Moore et al. [16] observed α week relaxation around the β region for higher-molecular weight polyethylenes with no branching. In contrast, the existence of β relaxation is well identified for branched polyethylenes. Klein et al. [17] proposed that the β relaxation was associated with the relaxation of short chain branches or the amorphous regions. These observations, together with thermal expansion measurements on high density and branched polyethylenes, led to the proposal that the β relaxation corresponds to the glass transition of semicrystalline polyethylene. According to Boyer [18], the β relaxation is postulated to be associated

* Corresponding author. Tel.: +81-761-51-1621; fax: +81-761-1625.
E-mail address: nitta@jaist.ac.jp (K.-h. Nitta).

0032-3861/01/$ - see front matter
PII: S0032-3861(00)00418-3

Table 1
Molecular characteristics of B-PE

Sample	SCB (mol%)	M_w ($\times 10^{-4}$)	M_w/M_n	Density (kg m^{-3})	χ_v [a]	T_m [b] (K)	L_p [c] (nm)	L_c [d] (nm)	L_a [e] (nm)
B-PE0	0	6.70	2.23	942	0.59	406	24.4	14.4	10.0
B-PE0.9	0.88	7.80	1.77	919	0.43	395	19.8	8.5	11.3
B-PE1.8	1.82	7.90	1.72	913	0.40	390	18.5	7.4	11.1
B-PE2.2	2.18	7.40	1.80	912	0.39	388	17.4	6.8	10.6
B-PE3.1	3.08	8.00	1.67	906	0.35	381	16.3	5.7	10.6
B-PE3.5	3.54	7.70	1.79	905	0.34	378	15.7	5.3	10.4

[a] Crystallinity in volume fraction.
[b] Melting temperature.
[c] Long period obtained by SAXS measurements.
[d] Lamellar thickness determined from $\chi_v L_p$.
[e] Amorphous layer thickness determined from $(1 - \chi_v)L_p$.

with α glass transition process of loose loop and intercrystalline tie molecules which are under more constraints. From a careful examination of the crystallinity dependence of the β relaxation process, Mandelkern et al. [19,20] demonstrated that the β relaxation results from the relaxation of chain units in the interfacial region.

The γ relaxation process in polyethylene has also been extensively studied by numerous investigators. Wada et al. [21] and Fischer et al. [22] attributed the γ relaxation to the motion of disordered chain segments at the surface of polymer crystals. Sinnott [23], Hoffman et al. [24], Pechhold et al. [15], and Iller [25] concluded that this relaxation arose at least in part for motion of defects in the crystalline regions. Regardless of the specific mechanism, these investigators consider the γ relaxation to arise from the crystal regions. On the other hand, according to Crissman [26], polycrystalline long-chain paraffins showed no γ relaxation peaks, suggesting that the γ relaxation is associated with small-scale motions within the amorphous component in polyethylene. In addition, Willbourn [27] showed that the γ relaxation process is assigned to the glass transition of methylene sequence and have the same effect as the brittle–ductile transition. Deniss [28] and Boyd et al. [29] arrived at the similar conclusion from the experimental results of the thermal expansion data and PVT data. Shatzki [30] and Boyer [31] attributed the γ relaxation to be a subglass relaxation which can be modeled in terms of crankshaft mechanism in which the five or three carbon bonds move as a crankshaft but the mechanism required a significant free volume being inhibited by the matrix [14]. These investigators believe that this relaxation corresponds to the glass transition of polyethylene. Thus, despite the extensive work that has been reported on polyethylene, there is no generally accepted explanation of the molecular origin for the γ relaxation.

As described above, the molecular interpretation for the mechanical relaxations has been elusive and controversial, although the extensive amount of experimental data on the dynamic mechanical properties has been done in the past. The reason for this situation seems to lie in the complication of the isolated structural variables, i.e. the polydispersity in composition and in molecular weight, which is a typical feature of the conventional polyethylenes used in the past. For example, Ziegler-catalyzed linear low-density polyethylenes are identified to be composite molecules of higher-molecular-weight homopolymers and lower-molecular-weight copolymers and/or stereoblock sequence of comonomer units forms along the methylene chain [32–34].

The discovery of highly active catalysts has led to the establishment of the single-site metallocene catalysts [35]. These catalysts yield polyolefins of most probable molecular weight distributions. The mechanism of occurrence of short chain branching is quite different between the metallocene-catalyzed polyethylenes and the conventional ones. The molecular weight distribution of the metallocene catalyzed polyethylenes is narrow and the comonomer

Table 2
Molecular characteristics of L-PE

Sample	$M_w \times 10^{-4}$	M_w/M_n	Density (kg m^{-3})	χ_v	L_p (nm)	L_c (nm)	T_m (K)
L-PE2.6	2.62	1.9	952	0.70	16.1	11.2	405
L-PE5.3	5.26	1.9	943	0.63	17.4	11.0	404
L-PE7.7	7.70	2.2	942	0.63	20.8	13.1	406
L-PE8.3	8.27	1.8	946	0.65	20.1	13.5	406
L-PE18	18.3	2.8	941	0.62	23.1	14.4	407
L-PE23	23.4	2.3	934	0.58	24.9	14.4	408
L-PE72	71.5	2.6	930	0.55	29.6	16.3	409
L-PE142	142.0	2.6	930	0.55	38.2	21.0	407
L-PE269	269.0	2.7	929	0.54	41.5	22.5	407

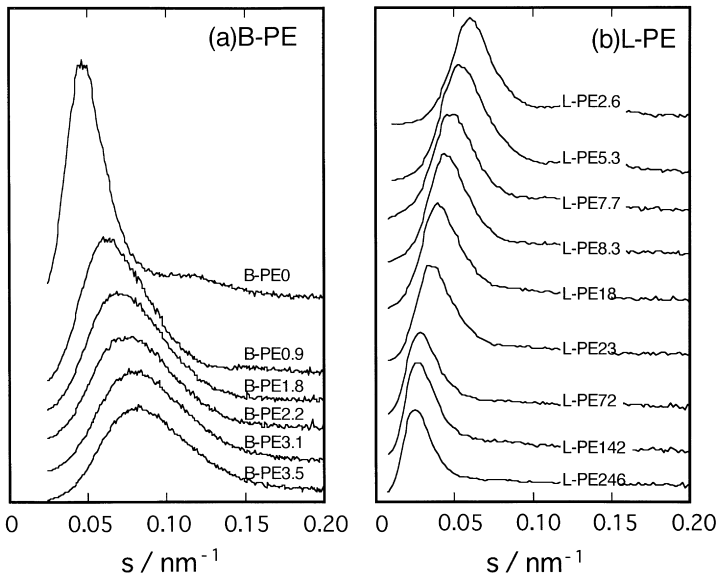

Fig. 1. Lorentz-corrected X-ray intensities scattered from B-PE and L-PE samples plotted against the wavenumber.

distribution is homogeneous [36,37]. In this work, we have studied the effects of molecular weight and short chain branching on dynamic mechanical properties for metallocene-catalyzed linear polyethylenes.

2. Experimental

2.1. Materials and sample preparation

Two different sets of linear polyethylenes prepared via a metallocene catalyst system were used in this work. The one is a series of linear polyethylenes with various molecular weight in the range from 2.5×10^4 to 260×10^4. The molecular characteristics of the polyethylene samples are given in Table 1. The weight and number average molecular weights were obtained by gel permeation chromatography. The nomenclature used is L-PE and its end numeral the molecular weight M_w in 10^4.

The other one is a type of polyethylenes with butyl branches, i.e. ethylen-1-hexcene copolymers, and with the same molecular weight. The molecular characteristics of the branched polyethylenes are given in Table 2. The comonomer contents were in the range 0–3.5 mol%. The co-unit content was determined by high-resolution ^{13}C NMR using established methods and assignments that are reported in the literature [38,39]. The nomenclature used is B-PE and its end numeral the average short chain branching SCB content in mol%.

These polyethylenes were melt pressed in a laboratory hot press at 463 K and at 10 MPa for 3 min. The sample specimens quenched at 273 K were prepared for the measurements. The thickness of the compression-molded samples was adjusted to a thickness suitable to the intended experiment.

2.2. Characterization

Differential scanning calorimetry (DSC) measurements were carried out using Mettler DSC820 calorimeter that was calibrated for temperature and melting enthalpy using indium as a standard. The samples of about 10 mg weight sealed in aluminum pans were heated from 223 to 423 K at a scanning rate of 10 K/min under a nitrogen atmosphere.

The density for all samples was measured at 303 K using the flotation method. The binary medium prepared from various ratios of distilled water and ethyl alcohol was used. The degree of crystallinity was calculated from a relationship with constants of 1000 and 856 kg/m^3 for the density of the crystalline and amorphous regions, respectively [40].

The small angle X-ray scattering (SAXS) measurement was performed with a point focusing optics and an one-dimensional position sensitive proportional counter (PSPC) with an effective length of 10 cm. The SAXS optics has a toroidal mirror and a crystal monochromator. The CuKα radiation supplied by a MAC Science M18X generator operating at 40 kV and 30 mA was used throughout. The distance between the sample and PSPC was about 40 cm. The geometry was further checked by a chicken tendon collagen, which gives a set of sharp diffractions corresponding to 65.3 nm.

The results of characterization of L-PE and B-PE samples are added in Tables 1 and 2, respectively.

2.3. Dynamic mechanical measurement

The measurements on the linear dynamic mechanical properties were made using a dynamic mechanical analyzer (Rheology Co. Ltd DVE V-4) on rectangular specimens of the following dimensions: length 20 mm, width 5 mm, and

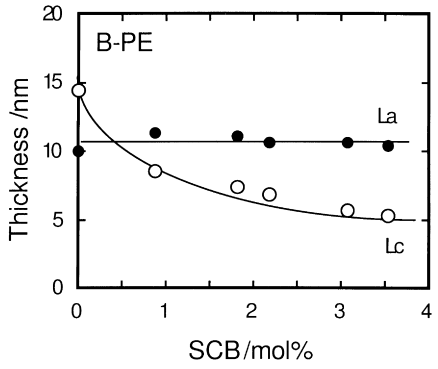

Fig. 2. Lamellar thickness Lc and amorphous layer thickness La plotted against the comonomer content for B-PE samples.

thickness around 0.5 mm. The measurements were made at a constant frequency of 10 Hz with a constant oscillation amplitude of 5 mm. The temperature dependences of the storage tensile modulus E' and loss modulus E'', and loss tangent tan δ were measured from 120 to 420 K at a heating rate of 2 K/min under a nitrogen atmosphere.

The activation energy for each relaxation process was obtained from the temperature dependence of the shift factor on the dynamic mechanical spectra around the corresponding relaxation temperature.

3. Results and discussion

3.1. Structural characteristics

Fig. 1 shows the Lorentz-corrected SAXS intensities plotted against the wavenumber $s(= 2/\lambda \sin \theta)$ in which 2θ is the scattering angle and λ the X-ray wavelength ($= 0.1542$ nm). The angular position of the intensity peak shifts toward larger s with the peak width being broad as the SCB content increases for B-PE systems. In contrast, the peak of L-PEs sharpened and significantly shifted to lower s with increasing molecular weight. The maximum point in the SAXS curves yields the average long period.

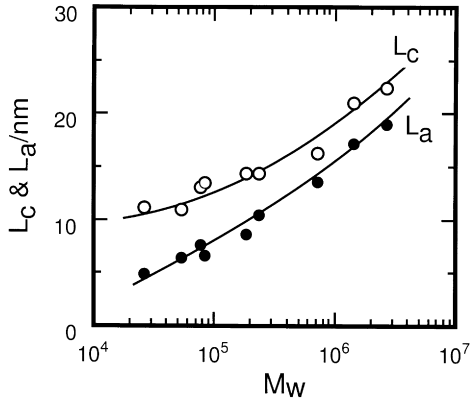

Fig. 3. Lamellar thickness Lc and amorphous layer thickness La plotted against the molecular weight M_w for L-PE samples.

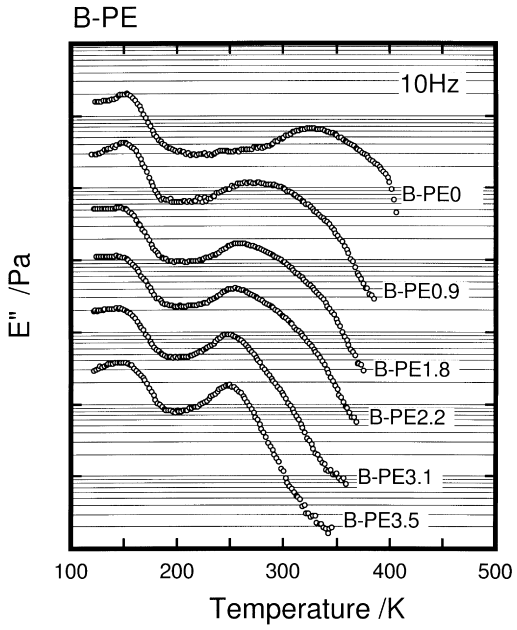

Fig. 4. Temperature dependence of tensile loss modulus E' at 10 Hz for B-PE samples.

The lamellar thickness and the amorphous layer thickness can be determined from data of volume fraction of crystals χ_v and the SAXS long period L_p. Structural characteristics for B-PE and L-PE samples are included in Tables 1 and 2, respectively. The introduction of noncrystallizing co-units into the chain leads to a continuous decrease in the degree of crystallinity with increasing SCB content at fixed molecular weight. Moreover, we find a significant decrease in the degree of crystallinity with increasing molecular weight for linear PE having no branching. It was found that the very large range in the degree of crystallinity that can be attained by control of molecular weight as well as comonomer content.

Although the increases in SCB and molecular weight lower the degree of crystallinity, the effects of SCB and molecular weight on lamellar morphology such as lamellar thickness and amorphous thickness is much different from each other. Fig. 2 demonstrates that as branch content increases, the lamellae become thinner but amorphous layer thickness remains constant. The metallocene-catalyzed PEs used in this work have narrow molecular weight distribution and homogeneous comonomer distribution. This is likely because the methylene stem length that is crystallizable is effectively reduced by the homogeneous introduction of α-olefin units. On the other hand, the data on lamellar morphology of L-PEs with no branches (see Fig. 3) showed that both crystal lamellar and amorphous layer thicknesses increase with increasing molecular weight. As is well known, the molecular weight influences not only the degree of crystallinity that can be achieved but also the rate of crystallization [41]. The increase in molecular weight makes it possible to increase the crystallizable methylene

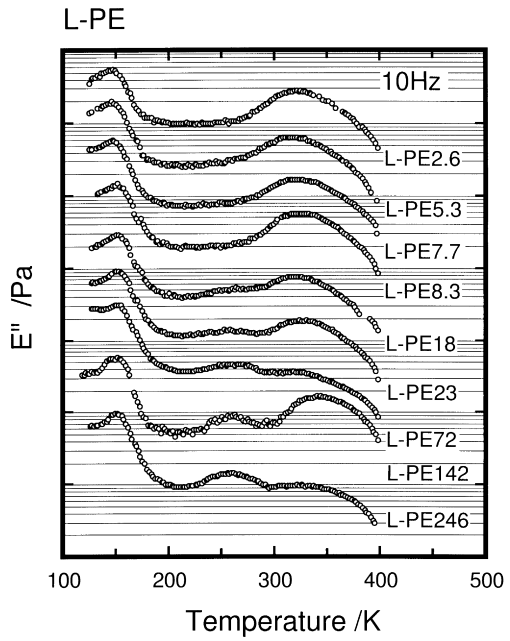

Fig. 5. Temperature dependence of tensile loss modulus E'' at 10 Hz for L-PE samples.

sequence, and this leads to thicker lamellae, whilst the increase in molecular weight restrains the crystallization rate because of molecular topological restrains such as chain intertwining and entanglements, resulting in the increase in the amorphous content.

3.2. Dynamic mechanical properties

The mechanical relaxation spectra of B-PE and L-PE systems are shown in the form of loss modulus in Figs. 4 and 5, respectively. Three relaxations were observed also for the metallocene-catalyzed PE series. Careful examination of the dynamic moduli data in the α relaxation region showed that there are two (α_1 and α_2) relaxations having different activation energies: the activation energies for the α_1 and α_2 relaxations were 80 and 100–120 kJ/mol, respectively, which are comparable with those of the conventional PEs [8].

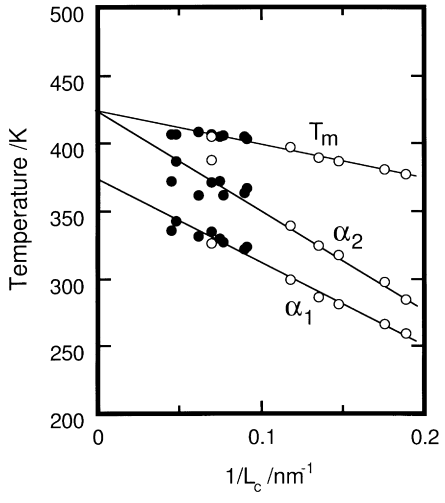

Fig. 6. Relaxation temperature of α_1 and α_2 processes and melting temperature plotted against inverse of lamellar thickness for (●) L-PE and (○) B-PE samples.

Fig. 6 demonstrates that a structural factor which governs relaxation processes of linear polyethylenes is the lamellar thickness. The temperature locations T_α of the α relaxations and the melting temperature T_m have qualitatively similar functional dependence of $1/L_c$. In addition, it was found that both lines for the α_2 peak temperature $T_{\alpha 2}$ and T_m extrapolate to 415 K which is identical with the equilibrium melting temperature T_m^0 of completely crystalline PE. It should be noted here that the slope of the line for $T_{\alpha 2}$ vs $1/L_c$ relation is three times larger than that for T_m vs $1/L_c$ relation. Therefore, considering that the lamellar thickness dependence of the melting temperature follows the Thompron–Gibbs equation, the following empirical equation for the α_2 peak temperature has the form:

$$T_{\alpha 2} = T_m^0\left(1 - 3\frac{2\sigma}{\Delta h_f L_c}\right) = T_m^0\left(1 - \frac{2\sigma}{(\Delta h_f/3)L_c}\right) \quad (1)$$

where σ is the surface free energy and Δh_f is the heat of fusion. The term of $\Delta h_f/3$ may result from the fact that the α_2 process is related with the one-dimensional thermal expansion of crystal lattice as demonstrated by Takayanagi et al. [12]. Consequently, we can obtain the following conventional equation:

$$T_{\alpha 2} = 2T_m - 3T_m^0 \quad (2)$$

The α and γ relaxations were also observed in all the samples but the β relaxation appear not only in the B-PE samples but also in the L-PE samples with molecular weights greater than 10^5. As seen in Figs. 4 and 5, the β peak is more evident as the SCB content and the molecular weight increase. However, the shape of the β peak of B-PE is somewhat different from that of high-molecular-weight L-PEs.

As shown in Fig. 7, the β relaxation temperature T_β of B-PE linearly decreases with decreasing L_c, reaching an extrapolated limiting value of 215 K which is identical with T_g of a completely amorphous ethylene-1-hexene copolymer (EHR) with 57 mol% 1-hexene [42]. The molecular motion in the amorphous layer is suggested to differ from those in completely amorphous polymer because of the restriction by the lamellar plates [43]. In the case of branched polyethylenes, these results support the idea that the β relaxation can be associated with molecular motions of the loose tie and loop chains with short chain branches confined between two adjacent lamellae.

On the other hand, T_β of high-molecular-weight L-PEs occur in the vicinity of 250–260 K and is almost invariant with the lamellar thickness. In addition, Fig. 8 shows that there are large differences in activation energies of shift factors between the β processes of B-PE0.9 and L-PE142.

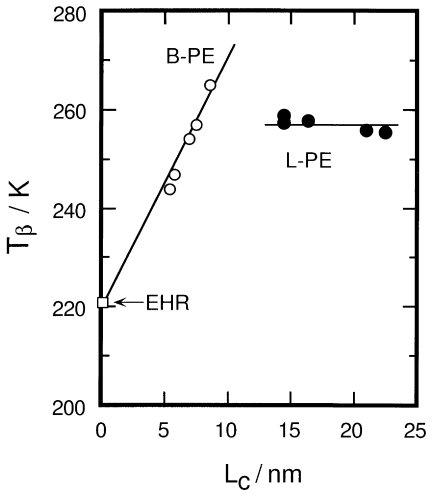

Fig. 7. Relaxation temperature of β plotted against lamellar thickness for (●) L-PE and (○) B-PE samples.

The β processes of B-PE0.9 and B-PE3.5 show 220 and 250 kJ/mol, respectively, which are comparable with that of EHR (200 kJ/mol), whilst the activation energy of L-PE142 was 90 kJ/mol. These results suggest that the molecular origin for the β process of L-PEs is quite different from that of B-PEs. Since formation of the loose tie and loop molecules in the amorphous layers is likely for higher-molecular-weight PEs, this behavior is consistent with the view that the β relaxation is the consequence of the motion of the loose tie molecules. The absence of the β relaxation in typical L-PE samples having a thinner amorphous layer thickness, which is considered to promote taut tie molecules, can be directly attributed to the lack of loose tie molecules. This is schematically presented in Fig. 9 for an amorphous layer of typical L-PE and high-molecular-weight L-PE. Therefore, the taut tie molecules cannot be relaxed prior to the α relaxation process. For examining the effects of taut tie molecules on the elastic modulus, the values of E' at which the γ dispersion is terminated

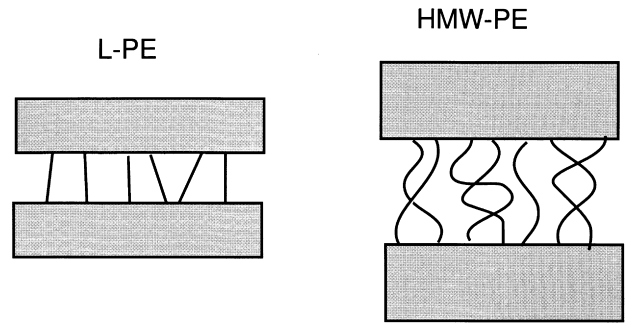

Fig. 9. Tie molecules in the amorphous layer between adjacent lamellae for typical L-PE and high-molecular-weight L-PE.

are plotted against $1/L_a$ in Fig. 10. It was found that the extrapolation values of the E'' at $1/L_\alpha = 0$ is accordance with the value of EHR. The important result is that the modulus is inversely proportional to the amorphous layer thickness. This may correspond to the fact that the plateau modulus on the stress relaxation behavior for a typical polymer liquid is inversely proportional to the molecular weight between chain entanglements. Thus, the proportionality as seen in Fig. 10 demonstrates the contribution of taut tie molecules to storage modulus according to analogy of the rubber-like response in the plateau region of the viscoelastic properties.

As seen in Figs. 4 and 5, the γ dispersion shifts to lower temperature and sharpen with decreasing SCB content and with increasing M_w. The position of the γ relaxation slightly increases with increasing L_c and the data are found to fall on one straight line as shown in Fig. 11. Extrapolation of T_γ value to a completely amorphous sample gives a value of 140 K, which corresponds to the glass transition temperature of amorphous methylene stems estimated by means of thermal expansion, compressibility, specific heat and dynamic mechanical data [29,44].

The primary relaxation associated with the glass transition of semicrystalline polymers can be explained by the molecular process of conformational changes in the

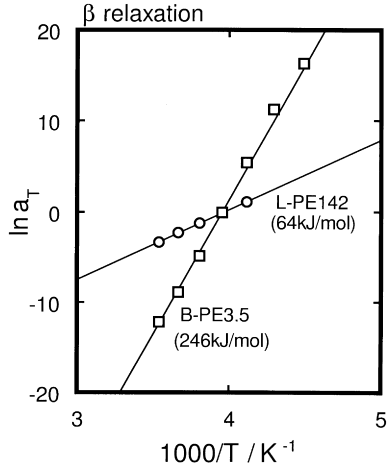

Fig. 8. Arrhenius plots of shift factors of B-PE3.5 and L-PE143.

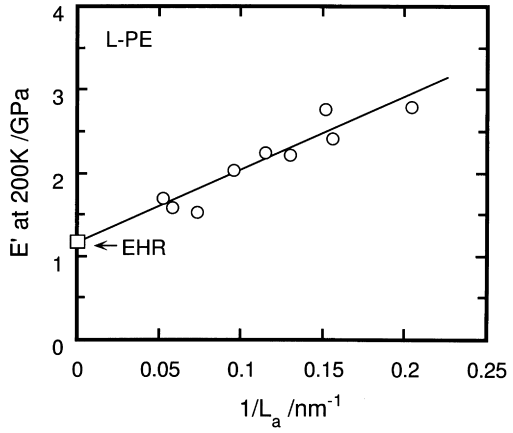

Fig. 10. Dynamic storage modulus E' after γ process inverse of against amorphous layer thickness for L-PE samples.

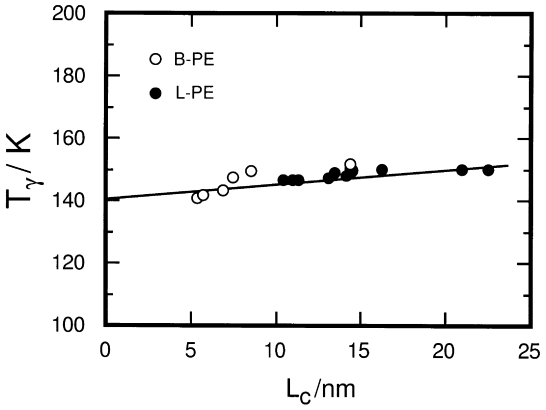

Fig. 11. Relaxation temperature of γ process plotted against lamellar thickness for (●) L-PE and (○) B-PE samples.

amorphous region. It is likely that the γ relaxation mechanism is associated with segmental motion of low-molecular-weight component such as floating and cilia chains in the amorphous layers as demonstrated by Boyer [18]. Therefore, we can propose that the methylene sequence affects the molecular motion of floating and cilia chains and thereby the position of the γ relaxation slightly shifts to higher temperature. In addition, it is assumed that the segmental relaxation of floating and cilia chains has the same effect as the glass transition in linear polyethylenes because these chains can be considered to be lower molecular weight molecules.

4. Summary

In this work, we have studied the molecular morphology and dynamic mechanical relaxation for two series of metallocene-catalyzed linear polyethylenes: one is the linear polyethylene with no branches having various molecular weight (L-PE) and the other is the linear polyethylenes (B-PE) having various degrees of short-chain branching. The important conclusion concerning the differences in the lamellar morphology between B-PE and L-PE is that M-PE shows a greater dependence of comonomer content on thinning of crystal lamellae, in which the amorphous layer thickness is independent of the SCB content. This will be because the methylene sequence, or crystallizable part, decreases as the comonomers are homogeneously incorporated into a main chain.

The relaxation behavior of linear polyethylene is strongly influenced by structural valuables that describe the crystalline-amorphous state. The main dynamic mechanical features of those new polyethylenes are the following:

(1) The structural factor that contributes to the α relaxation was found to be lamellar thickness. The α relaxation and melting temperatures have similar functional dependence of the inverse of the lamellar thickness.

(2) Although the β relaxation process appears in the high-molecular-weight L-PE samples as well as the B-PEs, the molecular mechanism underlying the β process was found to be quite different between B-PE and L-PE. The β process of high-molecular-weight L-PE is attributed to the glass transition of loose tie and loop molecules in the amorphous layers. In the case of B-PE, the β process is associated with molecular motion of the amorphous chains with branched portions restricted by lamellar crystals.

(3) The methylene segment affects the dispersion for both systems where the γ relaxation is more intensive and the position T_γ shifts to a lower temperature with the decreasingly methylene sequence and extrapolates to the glass transition of amorphous polymethylene. The γ relaxation can be associated with segmental motion of floating and cilia chains in the amorphous layer.

Acknowledgements

The authors thank Prof. S. Nojima of JAIST for his help with the SAXS measurements. The authors also thank Yokkaichi Research Laboratory of TOSOH Corporation for kindly supplying the experimental materials.

References

[1] Fatou JG, Maciá IG, Marco C, Gómez MA, Arribas JM, Fontecha A, Aroca M, Maritínez MC. J Mater Sci 1996;31:3095.
[2] Peacock AJ, Mandelkern L. J Polym Sci Polym Phys Ed 1990;28:1917.
[3] Mandelkern L. Polym J 1985;17:337.
[4] Hosoda S, Vermurer A. Polym J 1992;29:939.
[5] Capaccio G, Ward IM. J Polym Sci Polym Phys Ed 1984;22:475.
[6] McCrum NG, Moris EL. Proc R Soc London A 1966;292:506.
[7] Nakayasu H, Markritz J, Plazek DJ. J Trans Soc 1961;5:261.
[8] Kajiyama T, Okada T, Sakoda A, Takayanagi M. J Macromol Sci — Phys B 1973;7:583.
[9] Kyu T, Yasuda N, Suehiro S, Nomura S, Kawai H. Polym J 1976;8:565.
[10] Suehiro S, Yamada T, Inagaki H, Kyu T, Nomura S, Kawai H. J Polym Sci Polym Phys Ed 1979;17:763.
[11] Tanaka A, Chang EP, Delf B, Kimura T, Stein RS. J Polym Sci Polym Phys Ed 1973;11:1891.
[12] Takayanagi M, Aramaki T, Yoshino M, Hoashi H. J Polym Sci 1960;46:531.
[13] Mansfield M, Boyd RH. J Polym Sci Polym Phys Ed 1978;16:1227.
[14] Boyd RH. Polymer 1978;26:1123.
[15] Pechhold W, Eisele V, Knauss G. Kolloid Z 1978;196:27.
[16] Moore RS, Matsuoka S. J Polym Sci C 1963;5:163.
[17] Klein DE, Sauer JA, Woodward AE. J Polym Sci 1956;22:455.
[18] Boyer RF. J Macromol Sci — Phys B 1973;8:503.
[19] Popli R, Gordon M, Mandelkern L. J Polym Sci Polym Phys Ed 1984;22:407.
[20] Popli R, Mandelkern L. Polym Bull 1961;83:2057.
[21] Wada Y, Tsuge K, Arisawa K, Shisa K, Hotta Y, Hayakawa R, Nishi T. J Polym Sci C 1966;15:101.
[22] Fischer EW, Peterlin A. Makromol Chem 1964;74:1.
[23] Sinnott KM. J Appl Phys 1966;37:3385.

[24] Hoffman JD, Williams GW, Passaglia E. J Polym Sci C 1966;14:173.
[25] Iller VK. Rheol Acta 1964;3:202.
[26] Crissman JM. J Polym Sci Polym Phys Ed 1975;13:1407.
[27] Wollbourn AH. Trans Faraday Soc 1968;54:717.
[28] Deniss ML. J Appl Phys 1959;1:121.
[29] Sayer JA, Swanson SR, Boyd RH. J Polym Sci Polym Phys Ed 1978;16:1739.
[30] Shatzki TF. J Polym Sci 1962;57:496.
[31] Boyer RF. Rubber Rev 1963;34:1303.
[32] Shirayama K, Okada T, Kita S. J Polym Sci A 1965;3:907.
[33] Hosoda S. Polym J 1988;20:383.
[34] Wild L, Ryle TR, Knobeloch DC, Peat IR. J Polym Sci Polym Phys Ed 1982;20:441.
[35] Kamminsky W, Hahnsen H, Külper K, Wöldt R. US Patent 4, 1985: 542: 199.
[36] Heiland K, Kamminsky W. Makromol Chem 1992;193:106.
[37] Uozumi T, Soga K. Makromol Chem 1992;193:823.
[38] Randall JC. J Polym Sci Polym Phys Ed 1973;11:275.
[39] Hsieh ET, Randall JC. Macromolecules 1982;15:1402.
[40] Chiang R, Flory PJ. J Am Chem Soc 1961;83:2057.
[41] Mandelkern L. The crystalline state, 2nd ed. Washington, DC: ACS Book, 1993 (chap. 4).
[42] Yamaguchi M, Miyata H, Nitta K. J Appl Polym Sci 1996;62:87.
[43] Boyer RF. Macromolecules 1973;6:288.
[44] Stehling FC, Mandelkern L. Macromolecules 1996;3:242.